Acta Biomaterialia 10 (2014) 4639–4649

Contents lists available at ScienceDirect

Acta Biomaterialia

journal homepage: www.elsevier.com/locate/actabiomat

Biodegradable poly(ester urethane)urea elastomers with variable amino content for subsequent functionalization with phosphorylcholine

Jun Fang [a,b,c], Sang-Ho Ye [b,c], Venkat Shankarraman [b,c], Yixian Huang [d], Xiumei Mo [a,e], William R. Wagner [b,c,f,g,*]

[a] State Key Laboratory for Modification of Chemical Fibers and Polymer Materials, College of Materials Science and Engineering, Donghua University, Shanghai 201620, China
[b] McGowan Institute for Regenerative Medicine, University of Pittsburgh, Pittsburgh, PA 15219, USA
[c] Department of Surgery, University of Pittsburgh, Pittsburgh, PA 15219, USA
[d] Department of Pharmaceutical Sciences, School of Pharmacy, University of Pittsburgh, Pittsburgh, PA 15261, USA
[e] College of Chemistry and Chemical Engineering and Biological Engineering, Donghua University, Shanghai 201620, China
[f] Department of Chemical Engineering, University of Pittsburgh, Pittsburgh, PA 15219, USA
[g] Department of Bioengineering, University of Pittsburgh, Pittsburgh, PA 15219, USA

ARTICLE INFO

Article history:
Received 13 May 2014
Received in revised form 18 July 2014
Accepted 5 August 2014
Available online 14 August 2014

Keywords:
Biodegradable polyurethane
Bulk modification
Zwitterion
Cardiovascular biomaterial

ABSTRACT

While surface modification is well suited for imparting biomaterials with specific functionality for favorable cell interactions, the modification of degradable polymers would be expected to provide only temporary benefit. Bulk modification by incorporating pendant reactive groups for subsequent functionalization of biodegradable polymers would provide a more enduring approach. Towards this end, a series of biodegradable poly(ester urethane)urea elastomers with variable amino content (PEUU–NH_2 polymers) were developed. Carboxylated phosphorycholine was synthesized and conjugated to the PEUU–NH_2 polymers for subsequent bulk functionalization to generate PEUU–PC polymers. Synthesis was verified by proton nuclear magnetic resonance, X-ray photoelectron spectroscopy and attenuated total reflection Fourier transform infrared spectroscopy. The impact of amine incorporation and phosphorylcholine conjugation was shown on mechanical, thermal and degradation properties. Water absorption increased with increasing amine content, and further with PC conjugation. In wet conditions, tensile strength and initial modulus generally decreased with increasing hydrophilicity, but remained in the range of 5–30 MPa and 10–20 MPa, respectively. PC conjugation was associated with significantly reduced platelet adhesion in blood contact testing and the inhibition of rat vascular smooth muscle cell proliferation. These biodegradable PEUU–PC elastomers offer attractive properties for applications as non-thrombogenic, biodegradable coatings and for blood-contacting scaffold applications. Further, the PEUU–NH_2 base polymers offer the potential to have multiple types of biofunctional groups conjugated onto the backbone to address a variety of design objectives.

1. Introduction

Polyurethanes have been amongst the most extensively utilized synthetic polymers for biomedical applications, attractive for their mechanical properties and their ability to act as thermoplastic elastomers. More recently, a variety of new polyurethanes with designed degradability have been reported and explored for their use in regenerative medicine [1,2] and drug delivery systems [3–5]. Biodegradable polyurethanes are commonly designed with hydrolytically labile polyester macrodiol soft segments incorporated into the polymer backbone, such as with macrodiols of poly(lactic acid) (PLA), poly(glycolic acid) (PGA), polycaprolactone (PCL) [1], triblock copolymers of PCL–poly(ethylene glycol)–PCL [6,7] and other ester-containing copolymers [8,9]. In addition, enzymatically sensitive peptides can be incorporated into the hard segment to enhance degradation rates in response to enzymes that might be encountered in vivo [10,11]. Beyond their inherent design flexibility, linear biodegradable polyurethanes also are attractive for their ability to be processed into elastic scaffolds using a variety of techniques, including thermally induced phase separation, salt leaching, wet spinning, electrospinning and three-dimensional printing [1,7,12,13]. Furthermore, with mechanical properties that can approximate those of soft tissue, polyurethanes have been evaluated in many tissue environments, including nerve [14],

* Corresponding author at: Department of Bioengineering, University of Pittsburgh, Pittsburgh, PA 15219, USA. Tel.: +1 412 624 5324; fax: +1 412 624 5363.
E-mail address: wagnerwr@upmc.edu (W.R. Wagner).

http://dx.doi.org/10.1016/j.actbio.2014.08.008
1742-7061/

cartilage [13], ligament [15], abdominal wall [16], blood vessel [17] and cardiac wall [18,19].

Although significant progress has been made in the development of an array of biodegradable polyurethanes for biomedical applications, fewer reports have sought to develop biodegradable polyurethanes that incorporate pendant reactive groups for subsequent functionalization. Such polyurethanes would be useful to impart specific functionality for favorable cell behavior in tissue engineering scaffold applications [20,21] or for incorporating targeting moieties for drug delivery systems [4]. For degradable polyurethanes that would be in blood contact, functionalization of the backbone with non-thrombogenic groups, such as zwitterionic compounds [22–24], could be beneficial. For applications such as a scaffold for a tissue engineered blood vessel or a drug-eluting coating for a vascular stent, this latter type of polymer might be ideal.

The objective of this study was to synthesize and characterize a series of biodegradable elastomeric poly(ester urethane)ureas (PEUUs) that incorporated varying contents of pendant amino groups (PEUU–NH_2 polymers), which would be available for subsequent functionalization. To examine one specific type of functionalization, a carboxylated phosphorycholine derivative (PC–COOH) was conjugated to the PEUU–NH_2 polymers as a zwitterionic moiety that would be expected to increase the non-thrombogenic character of the base polymer and may also act to reduce smooth muscle cell proliferation. The effect of varying amine content in the PEUU–NH_2 polymers, and thus the amount of PC–COOH that could be incorporated in the modified polymers, was examined in terms of polymer physical properties, acute thrombogenicity and support of smooth muscle cell proliferation.

2. Materials and methods

2.1. Materials

Polycaprolactone diol (PCL, Mn = 2000), N-Boc-serinol (97%), 1,4-diisocyanatobutane (BDI), putrescine, stannous octotate ($Sn(Oct)_2$), 3-mercaptopropionic acid (MPA ⩾ 99%), N-(3-dimethylaminopropyl)-N′-ethylcarbodiimide hydrochloride (EDC), N-hydroxysuccinimide (NHS), trifluoroacetic acid (TFA), lipase from *Thermomyces lanuginosus* (⩾100,000 U g^{-1}) and MTT dye solution (3-(4,5)-dimethylthiazol (-2-y1)-2,5-diphenyltetrazolium bromide) were purchased from Sigma-Aldrich and used as received, except where mentioned otherwise. PCL was dried in a vacuum oven at 60 °C overnight to remove residual water before synthesis. BDI and putrescine were purified using vacuum distillation before usage. 2-Methacryloyloxyethyl phosphorylcholine (MPC) was kindly provided by Prof. Kazuhiko Ishihara at the University of Tokyo.

2.2. Synthesis of PEUU with amino groups (PEUU–NH_2)

To prepare a poly(ester urethane)urea with controlled amino group content (PEUU–NH_2), PEUU polymers with protected amino groups (PEUU–Boc) were first synthesized from PCL diol and N-Boc-serinol, BDI, and a putrescine chain extender, then the amino groups were generated by a de-protection process (Fig. 1A). The synthesis was as follows: PCL diol and N-Boc-serinol were dissolved in anhydrous dimethylsulfoxide (DMSO, Sigma) in a three-necked flask with the concentration at 10% (w/v) and BDI was added under argon protection, followed by the addition of $Sn(Oct)_2$ (0.05 wt.% with respect to the monomer). The reaction was carried out for 3 h at 80 °C and then cooled to room temperature. Putrescine/DMSO solution at 2% (w/v) was added dropwise to the prepolymer solution. The molar ratio of (PCL with N-Boc-serinol)/BDI/putrescine was 1:2:1 and the final polymer solution concentration was ~5% (w/v). The reaction continued for 18 h with stirring at 40 °C. The polymer was precipitated in deionized water (DI water), then immersed in isopropanol for further purification over 1 day, and dried in a vacuum oven at 60 °C for 2 days. The yield of PEUU–Boc was ~90%.

The synthesized PEUU–Boc (8 g) was dissolved to a concentration of 5% (w/v) in 160 ml chloroform/TFA (50/50) in a round bottom flask and stirred for 1 h at room temperature to remove the Boc-protected groups. The excess TFA and chloroform were moved by rotary evaporation and the polymer was precipitated and neutralized in 2% (w/v) Na_2CO_3 aqueous solution (pH = 11.4) to remove residual TFA. The product was then washed with DI water and rinsed in isopropanol for 1 day, followed by drying in a vacuum oven at 60 °C for 2 days. The yield was greater than 92%. By controlling the molar ratio of PCL:N-Boc-serinol (1:1, 1:2, 1:3, 1:5 and 1:10), different numbers of Boc-protected amino groups could be incorporated into the PEUU polymers. These polymers were designated PEUU–Boc1, PEUU–Boc2, PEUU–Boc3, PEUU–Boc5 and PEUU–Boc10, respectively, based on this ratio. After deprotection of Boc, the PEUU–NH_2 polymers were designated PEUU–N1, PEUU–N2, PEUU–N3, PEUU–N5 and PEUU–N10, similarly based on the original Boc ratio. As a control, PEUU was synthesized with only PCL as a soft segment in the prepolymer synthesis step, as previously described [25].

2.3. Synthesis of a carboxylated phosphorycholine derivative (PC–COOH)

A carboxylated phosphorycholine derivative (PC–COOH) was synthesized by a thiol-ene reaction between MPA and MPC (Fig. 1B). The synthesis procedure was as follows: a round-bottom flask equipped with a magnetic stirrer was charged with anhydrous methanol (100 ml) after adding MPC (10 mmol, 2.96 g) and MPA (100 mmol, 8.64 ml). After argon injection for 5 min to remove the air, the flask was sealed and placed in a UV crosslinker (CL-1000 Model, Ultra-Violet Products Ltd, Upland, CA) which provided UV exposure (150 mJ cm^{-2}, 254 nm) for 3 h with stirring. After the reaction, the excess solvent was evaporated from the reaction mixture using a rotary evaporator and the product was precipitated using an anhydrous dimethyl ether/chloroform mixed solvent (50/50) to remove unreacted monomer. The obtained product was dried in a vacuum oven and the chemical structure of PC–COOH was confirmed by proton nuclear magnetic resonance (^{1}H NMR) (in DMSO-d_6); the peaks were: δ (ppm) 1.14 (α-CH_3CH—), 1.25 (α-CH_3), 2.51(—CH_2CH_2S), 2.56–2.75 (—$CH_2CH_2SCH_2$CH), 3.14(—$CH_2N(CH_3)_3$), 3.56 (—$CH_2N(CH_3)_3$), 3.86 (—OCH_2—), 4.10 (—$CH_2PO_4CH_2$—) and a broad peak for the carboxyl group at 13.5 (—COOH). The PC–COOH was successfully purified, and the signals from unreacted double bonds (—C═C—, 5.5–6.0 ppm) were not observable on the ^{1}H NMR spectrum (Supplemental Fig. S.1).

2.4. Preparation of PEUU modified with PC groups (PEUU–PC)

PEUU–PC polymers were obtained by conjugating the PC–COOH onto amine groups in PEUU–NH_2 through an EDC/NHS condensation reaction (Fig. 1C). It was theoretically determined that 2.83 g of PEUU–N1 contained 1 mmol NH_2, and this amount was completely dissolved in 14 ml DMSO solvent at 90 °C and then cooled to room temperature. The molar ratios of reaction reagents used for the various synthesized polymers, together with the theoretical molecular weight of a polymer unit, and hard segment content, are provided in the Supporting Information as Table S.1.

PC–COOH (2 equivalents of NH_2, 2 mmol, 0.802 g) was reacted with NHS (3 equivalents of NH_2, 3 mmol, 0.345 g) and EDC (3 equivalents of NH_2, 3 mmol, 0.575 g) in 10 ml DMSO at room

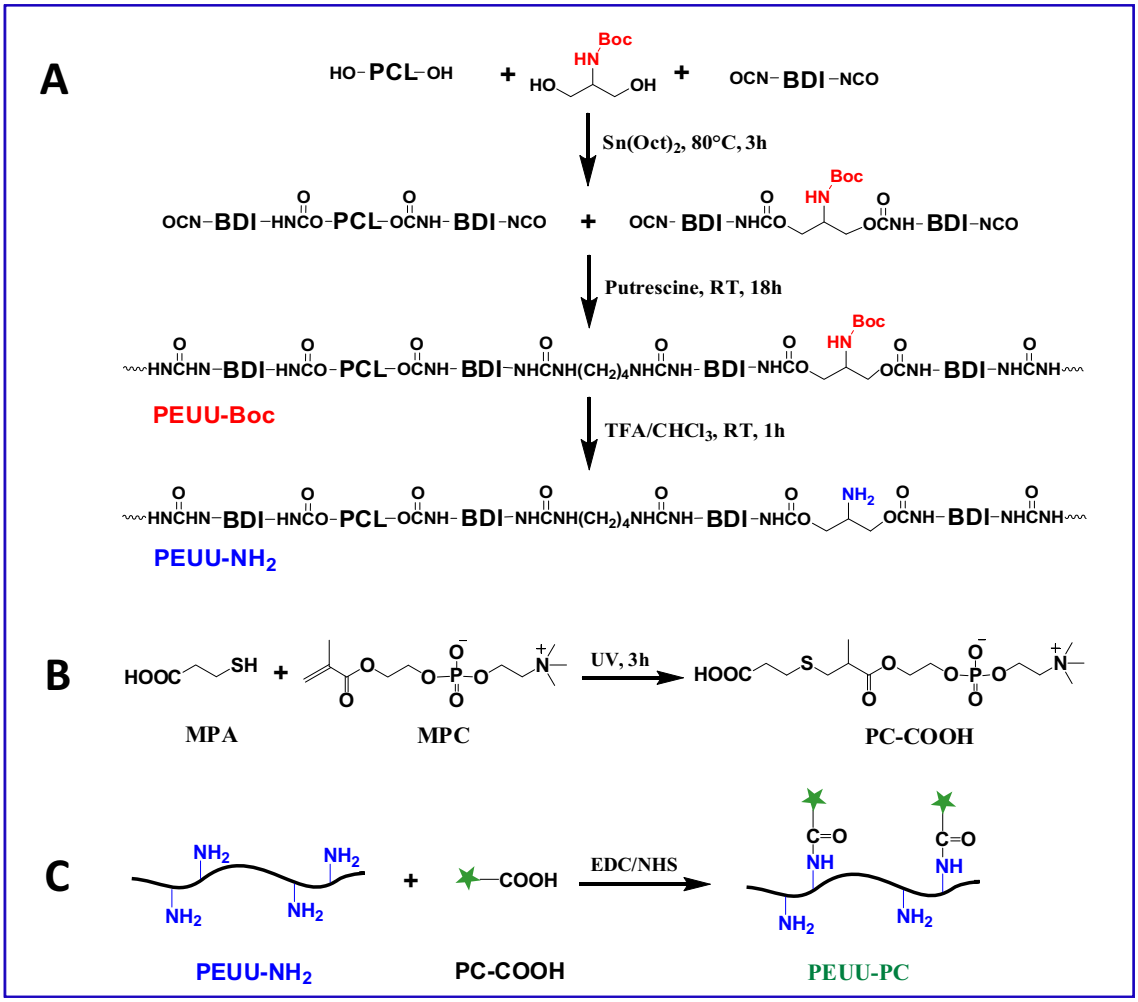

Fig. 1. Schematic for synthesis of (A) poly(ester urethane)urea containing amino groups (PEUU-NH2), (B) PC-COOH and (C) PEUU-PC.

temperature overnight under an argon atmosphere. The reaction mixture was then added to the dissolved PEUU–NH_2 solution, followed by stirring for another 2 days at room temperature under argon. For polymer precipitation, the polymer solution was poured into ethylene ether. The product was then washed with DI water and rinsed in isopropanol for 1 day and dried in a vacuum oven at 60 °C for 2 days. The yield was ~80%.

Films of all polymers were generated by solvent casting using 1,1,1,6,6,6-hexafluoroisopropanol (HFIP, Oakwood, Inc.) as a solvent followed by air drying in a fume hood for more than 1 day, and placement in a vacuum oven at room temperature for 2 days.

2.5. Polymer characterization

Polymer chemical structure was characterized by ^{1}H NMR (300 MHz, Bruker Biospin Co., Billerica, MA) using DMSO-d_6 as a solvent. Fourier transform infrared (FTIR) spectra were recorded on a Thermo Nicolet iS10 spectrometer equipped with a diamond Smart iTR. Polymer surface composition was analyzed by X-ray photoelectron spectroscopy (XPS) using a Surface Science Instruments S-probe spectrometer with a take-off angle of 55° (performed at NESAC-BIO, University of Washington). The surface composition of a given sample was averaged from three composition spots and the mean value for three different samples was determined. Thermal properties were measured by differential scanning calorimetry (DSC, DSC-60, Shimazu) at a scanning range of −100 to 200 °C with the temperature changing at a rate of 10 °C min^{-1} under nitrogen flow. During the test, each sample was heated to 200 °C, kept at 200 °C for 3 min to eliminate thermal history, cooled to −100 °C then heated to 200 °C again, and the second cycle was recorded. The glass transition temperature (T_g) was taken as the inflection of the DSC curve and the melting temperature (T_m) was taken as the peak temperature of the endothermic peak.

To visualize the formation and consumption of amino groups during the process of deprotection and modification, respectively, a ninhydrin assay (Sigma) on cast films (8 mm diameter) of PEUU–Boc, PEUU–NH_2 and PEUU–PC was performed. All films were immersed in 0.2 mol l^{-1} ninhydrin in ethanol solution at 60 °C for 20 min, and macroscopic images were then captured with a Nikon camera.

2.6. Tensile mechanical testing

Strips (2 × 20 mm) were cut from the polymer cast films and mechanical properties were measured on an MTS Tytron 250 MicroForce Testing Workstation at room temperature with a crosshead speed of 25 mm min^{-1} according to ASTM D638-98. For wet mechanical properties of PEUU–NH_2 and PEUU–PC films, the strips were immersed in DI water (37 °C) for 24 h, and tested immediately following removal from the water at room temperature. Four samples were tested for each polymer.

2.7. Water absorption and polymer degradation in PBS and lipase solution

Water absorption was defined in terms of the difference of the wet mass (w_2) and dry mass (w_1) of the film:

$$\text{Water absorption ratio } (\%) = 100 \times (w_2 - w_1)/w_1$$

Three independent measurements were performed on samples with dimensions of 10 × 10 × 0.2 mm.

Polymer degradation behavior after exposure to hydrolytic and enzymatic environments was quantified by dry weight loss. For hydrolysis, the weighed polymer film (W_0) was immersed in 10 ml of PBS at 37 °C. At each time point, the sample was rinsed with DI water (3×) and dried in a vacuum oven at 60 °C for 3 days, followed by weighing (W_1). For enzymatic degradation, the weighed polymer film (W_0) was placed in 2 ml of 100 U ml^{-1} lipase/PBS solution at 37 °C. The lipase/PBS solution was replaced with a fresh solution every 3 days. At each time point, the sample was rinsed in DI water (3×), dried in a vacuum oven at 40 °C for 3 days and then weighed (W_1). Three samples (10 × 10 × 0.2 mm) were used for each polymer at each time point. The mass remaining was calculated by the following formula:

$$\text{Mass remaining } (\%) = W_1/W_0 \times 100\%$$

2.8. In vitro blood contacting test

Whole ovine blood was collected by jugular venipuncture using an 18 gauge 1 1/2″ needle directly into a syringe after discarding the first 3 ml. NIH guidelines for the care and use of laboratory animals were observed, and all animal procedures were approved by the Institutional Animal Care and Use Committee (IACUC) at the University of Pittsburgh. The blood was quickly distributed into S-Monovette® tubes (3 ml; Sarstedt, Germany) containing sodium citrate. Thrombotic deposition on the polymer surfaces was assessed in vitro by employing a simple rocking test. Cast polymer films (~200 μm thick) were used to punch 10 mm diameter disks, washed in 70% ethanol for 15 min followed by DI water. Each disk was placed into a Vacutainer tube (Becton-Dickinson, with no additives) filled with 4 ml of fresh, citrated ovine blood and incubated for 3 h at 37 °C on a hematology mixer (Fisher Scientific). After ovine blood contact, surfaces were rinsed 10× with PBS and immersed in a 2.5% glutaraldehyde solution for 2 h at 4 °C to fix the platelets deposited on the surface. Then, the polymer film samples were serially dehydrated with increasing ethanol solutions, and sputter-coated with gold/palladium. Each sample surface was observed by scanning electron microscopy (SEM; JSM-6330F, JEOL USA). In samples not prepared for electron microscopy, deposited platelets on each surface were quantified by a lactate dehydrogenase (LDH) assay [26] with an LDH Cytotoxicity Detection Kit (Clontech Laboratories).

2.9. Rat vascular smooth muscle cell growth

A series of 6 mm diameter polymer disks were exposed to UV irradiation for sterilization (30 min per side, placed 60 cm from the 30 W UV lamp in a vertical flow laminar cabin), then washed with PBS and placed in the well bottoms of a 96-well cell culture plate, followed by seeding with 2000 cells per well of primary rat vascular smooth muscle cells (rSMCs) in 200 μl of cell culture medium (Dulbecco's modified Eagle's medium, DMEM) supplemented with 10% fetal bovine serum and 1% penicillin/streptomycin solution. The cell culture medium was exchanged every 3 days. Wells without a polymer disk added (designated TCPS) served as control. The MTT assay was conducted to measure rSMC metabolic activity. For each group, three samples were used in parallel. A live/dead kit (LIVE/DEAD Viability/Cytotoxicity Kit, Invitrogen Inc.) was also employed to stain rSMCs at each time point, and images were taken using fluorescence microscopy (Eclipse Ti, Nikon) to visualize relative cell numbers and to detect dead cells.

2.10. Statistical analyses

All results are represented as mean ± standard deviation. The data were analyzed by one-way analysis of variance, followed by Tukey's test for the evaluation of specific differences with Origin Pro 8. $p < 0.05$ was considered to represent a significant difference.

3. Results

3.1. Polymer characterization

The chemical structures of polymers were confirmed by ^{1}H NMR analysis. The ^{1}H NMR spectra of PEUU–Boc1, PEUU–N1 and PEUU–PC1 are seen shown in Fig. 2. PEUU–Boc1 showed a strong signal at 1.38 ppm assigned to methyl protons in the Boc groups. This peak disappeared completely in PEUU–N1 after deprotection. A specific chemical shift appeared in PEUU–PC1 at 3.14 ppm assigned to the peak —N(CH$_3$)$_3$ in PC groups after PC modification. The modification yield was determined to be more than 80% based on integration of peaks for —N(CH$_3$)$_3$ in PC and —CH$_2$CO in PCL. The peak of Boc at 1.38 ppm became stronger with more Boc-N-serinol in PEUU–Boc, while this chemical shift was not observed on the spectra of PEUU–NH$_2$. Similarly, the chemical peak of —N(CH$_3$)$_3$ in PC group also became stronger with increasing PC groups. The surface composition analysis by XPS (Table 1) also supports the presence of the PC groups, and showed that phosphorus (P) composition was 0.3% for PEUU–PC1, 0.7% for PEUU–PC3 and 0.9% for PEUU–PC5. The increase in sulfur (S) content on the PEUU–PC surfaces also suggested that the PC–COOH obtained from the thiol-ene reaction had led to successful engraftment onto PEUU–NH$_2$.

Attenuated total reflection Fourier transform infrared spectroscopy (ATR-FTIR) results (Fig. 3) further confirmed the chemical structure of the polymers. PEUU–PC exhibited the strong peak at 965 cm^{-1} which was assigned to the —N(CH$_3$)$_3$ vibration of PC. This signal became stronger as the content of PC groups in PEUU increased. The ninhydrin assay (Supplemental Fig. S.2) provided visual evidence of the deprotection and modification process. PEUU–Boc appeared white or light in color and became blue after deprotection generated PEUU–NH$_2$. Increasing the NH$_2$ density in PEUU–NH$_2$ resulted in a darker blue surface. The PEUU–PC became lightly colored again after PC modification, but noticeably more blue than the corresponding PEUU–Boc.

Water absorption of the cast films is shown in Table 2, where PEUU–NH$_2$ polymers increased in absorption modestly with increasing amine content, from 2.6% for PEUU–N1 to 12.2% for PEUU–N10 ($p < 0.05$). PEUU–PC polymers exhibited more hydrophilicity than the corresponding PEUU–NH$_2$ polymers, with water absorption increasing with PC content, from 17.3% for PEUU–PC1 to 38.4% for PEUU–PC5 ($p < 0.05$).

3.2. Mechanical and thermal properties

Representative tensile stress–strain curves of the dry and wet PEUU–NH$_2$ and PEUU–PC polymer films are shown in Fig. 4, with average mechanical parameters summarized in Table 2. Under dry conditions, the strain at break of PEUU–NH$_2$ polymers gradually decreased with increasing amine content, from 823% for PEUU–N1, to 246% for PEUU–N10 ($p < 0.05$). PEUU–PC polymers

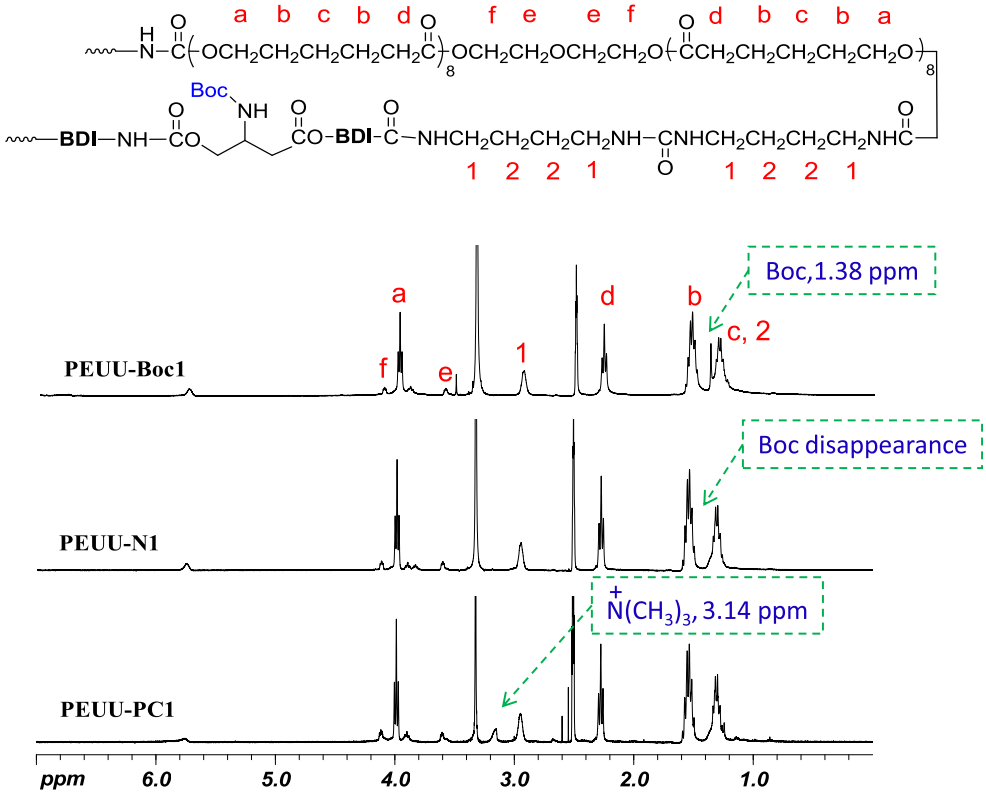

Fig. 2. ^{1}H NMR spectra of PEUU–Boc1, PEUU–N1, PEUU–PC1; DMSO-d_6 as solvent.

Table 1
Surface composition analysis of polyurethane films.

Samples	C	O	N	S	P
PEUU-N1	74.3 ± 3.7	20.5 ± 1.3	3.3 ± 0.1	0.0 ± 0.0	0.0 ± 0.0
PEUU-N3	66.8 ± 5.2	22.7 ± 1.0	5.7 ± 0.4	0.0 ± 0.0	0.0 ± 0.0
PEUU-N5	63.7 ± 1.1	23.8 ± 0.8	8.1 ± 0.8	0.0 ± 0.0	0.0 ± 0.0
PEUU-PC1	70.0 ± 3.5	23.6 ± 2.5	3.1 ± 1.1	0.1 ± 0.1	0.3 ± 0.1
PEUU-PC3	68.5 ± 0.7	23.5 ± 0.5	6.1 ± 0.4	0.6 ± 0.1	0.7 ± 0.1
PEUU-PC5	67.5 ± 0.8	22.5 ± 1.0	7.7 ± 0.1	0.9 ± 0.1	0.9 ± 0.1

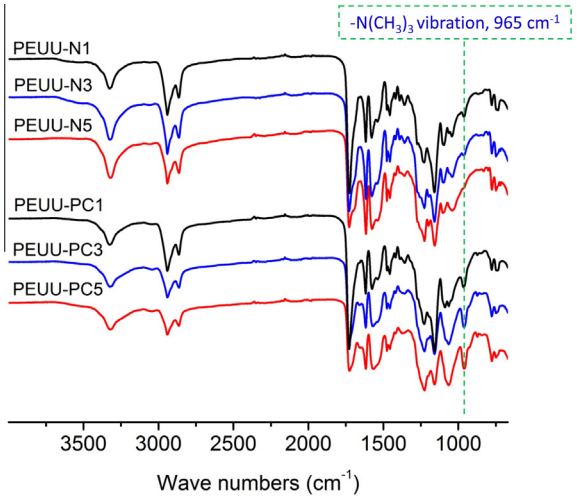

Fig. 3. ATR-FTIR spectra of PEUU–NH_2 and PEUU–PC.

tended to have elongations less than or equal to the equivalent amine containing polymer. PEUU–PC polymers showed higher tensile strengths (38 to 41 MPa) relative to corresponding PEUU–NH_2 polymers ($p < 0.05$). The initial modulus of PEUU–NH_2 also increased with increasing amino content in the PEUU–NH_2, and the PEUU–PC polymers showed the same tendency ($p < 0.05$). Under wet conditions, the strain at break of PEUU–NH_2 and PEUU–PC polymers were significantly decreased compared with their respective dry films. Tensile strength and initial modulus generally decreased with increasing hydrophilicity, but remained in the range of 5–30 MPa and 10–20 MPa, respectively. The tensile strength and initial modulus of PEUU–N1 changed little, while for PEUU–PC1 and the other PEUU–NH_2 and PEUU–PC polymers, these parameters significantly decreased.

DSC data are shown in Fig. 5 and exhibit the crystalline and glass-transition properties of PEUU–NH_2 (Fig. 5A) and PEUU–PC (Fig. 5B) polymers. The melting peaks became broader with increasing the NH_2 density and disappeared for PEUU–N5 and PEUU–N10. PEUU–PC showed the same tendency. All polymers showed a T_g for the soft segment at ~−60 °C.

3.3. Polymer degradation in PBS and lipase solution

Polymer degradation was evaluated in both PBS and lipase solution at 37 °C (Fig. 6). For hydrolytic degradation in PBS (Fig. 6A), PEUU–NH_2 polymers showed minimal degradation over the 16 week period, as did PEUU–PC1. However, at 16 weeks PEUU–PC3 and PEUU–PC5 degraded to a greater extent and differed significantly from PEUU–N3 and PEUU–N5, respectively. In the enzymatic degradation test with lipase (Fig. 6B), PEUU–NH_2 polymers showed greater degradation than in the PBS solution, while PEUU–PC polymers degraded to a comparable extent in the lipase solution as in PBS.

Table 2
Mechanical properties of PEUU–NH_2 and PEUU–PC under dry and wet conditions, and water absorption of dry films.

Polymer	Strain at break (%)		Tensile strength at break (MPa)		Initial modulus (MPa)		Water absorption (%)
	Dry	Wet	Dry	Wet	Dry	Wet	
PEUU-N1	823 ± 27[a]	693 ± 35[b]	25.5 ± 6.7[a]	29.8 ± 3.0[a]	13.0 ± 2.7[ab]	15.0 ± 1.6[a]	2.6 ± 0.4[a]
PEUU-PC1	735 ± 14[b]	485 ± 35[c]	38 ± 1.4[a]	13.6 ± 1.1[b]	15.2 ± 1.2[a]	10.3 ± 0.5[b]	17.3 ± 0.6[b]
PEUU-N2	685 ± 20	–	30.4 ± 3.6	–	18.8 ± 2.8	–	4.6 ± 1.1
PEUU-N3	600 ± 24[a]	530 ± 15[b]	34.4 ± 1.8[b]	28.1 ± 2.1[c]	26.6 ± 2.6[a]	17.3 ± 1.7[b]	7.8 ± 1.0[a]
PEUU-PC3	508 ± 26[b]	421 ± 30[c]	41 ± 3.0[a]	15.0 ± 2.8[d]	27 ± 3.1[a]	10.7 ± 0.9[c]	27.0 ± 1.5[b]
PEUU-N5	370 ± 17[a]	153 ± 40[b]	29.6 ± 2.8[b]	10.1 ± 2.3[c]	49.0 ± 3.5[a]	20.1 ± 2.6[b]	8.8 ± 0.8[a]
PEUU-PC5	370 ± 19[a]	110 ± 23[b]	38 ± 4.2[a]	5.3 ± 0.5[c]	43 ± 2.3[a]	10.7 ± 0.9[c]	38.4 ± 0.9[b]
PEUU-N10	246 ± 27	–	35.4 ± 2.7	–	140.6 ± 12.3	–	12.2 ± 0.7

Statistical comparisons were made amongst each PEUU-NH_2 type with a corresponding PEUU-PC type under dry and wet conditions. a, b, c and d denote statistically distinct groups for each measured parameter, including dry & wet, within a given set of PEUU-NH_2 and corresponding PEUU-PC polymers.

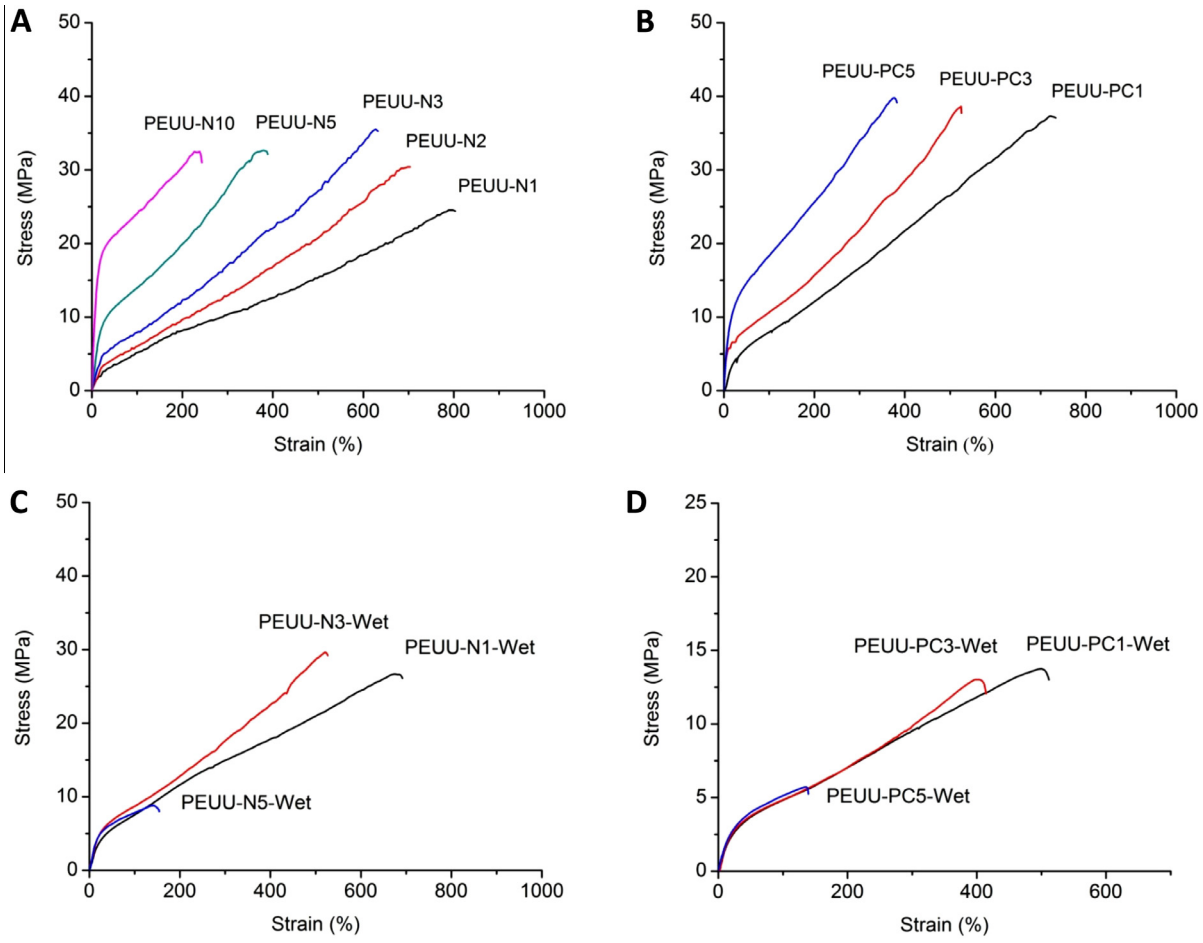

Fig. 4. Typical stress–strain curves of cast polyurethane films under dry conditions: (A) PEUU–NH_2, (B) PEUU–PC; and wet conditions: (C) PEUU–NH_2–Wet, (D) PEUU–PC–Wet, immersed in water (37 °C) for 24 h.

3.4. In vitro platelet deposition

In Fig. 7 scanning electron micrographs of polymer film surfaces following 3 h ovine blood contact showed similar levels of platelet deposition onto control PEUU and PEUU–N3 films with some of the deposited platelets extending pseudopodia. Platelet deposition onto PEUU–N1 and PEUU–N5 (data not shown) experienced similar levels of platelet deposition as visualized by SEM. In contrast, platelet deposition onto the PEUU–PC polymers was markedly reduced (Fig. 7), with sparse deposition of individual platelets observed. Quantification of platelet deposition using the LDH assay (Fig. 8) confirmed the visual results, with PEUU–PC polymers exhibiting significantly lower platelet deposition than PEUU and PEUU–N3.

3.5. rSMC growth

The ability of the surfaces of PEUU, PEUU–N3, PEUU–PC1, PEUU–PC3, PEUU–PC5 and TCPS to support primary rSMC growth is seen in Fig. 9 with live/dead cell staining at days 2 and 4. Clear differences in cell numbers on the surfaces are seen between the PEUU–PC polymers and the PEUU–N3, PEUU and TCPS control surfaces, with the latter supporting cell adhesion and proliferation between days 2 and 4. In support of this visual trend, the MTT assay, which measures mitochondrial activity (Fig. 10), quantitatively demonstrated the differences between the surfaces. At day 2, while PEUU, PEUU–N3 and PEUU–PC1 were statistically equivalent, PEUU–PC3 and PEUU–PC5 had lower relative mitochondrial

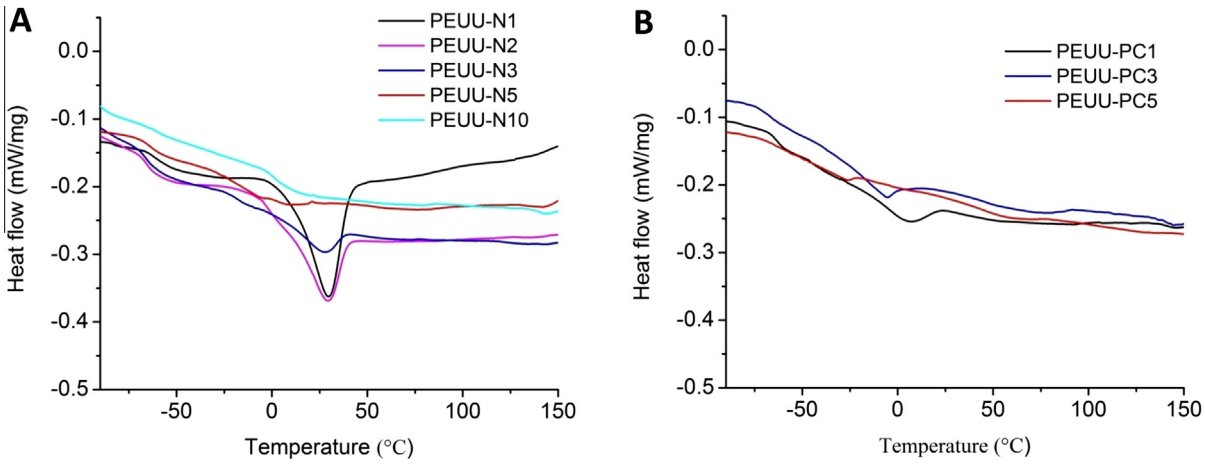

Fig. 5. DSC analysis of polyurethanes (second cycle): (A) PEUU–NH_2; (B) PEUU–PC.

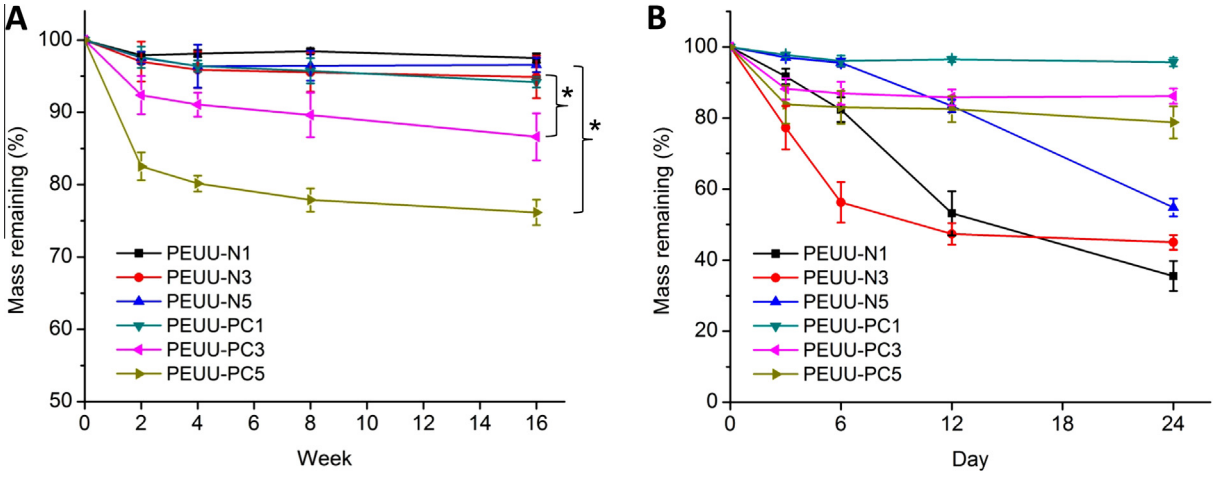

Fig. 6. Mass remaining for cast films of PEUU–NH_2 and PEUU–PC in (A) PBS and (B) 100 U ml^{-1} lipase in PBS solution at 37 °C; $^{*}p < 0.05$.

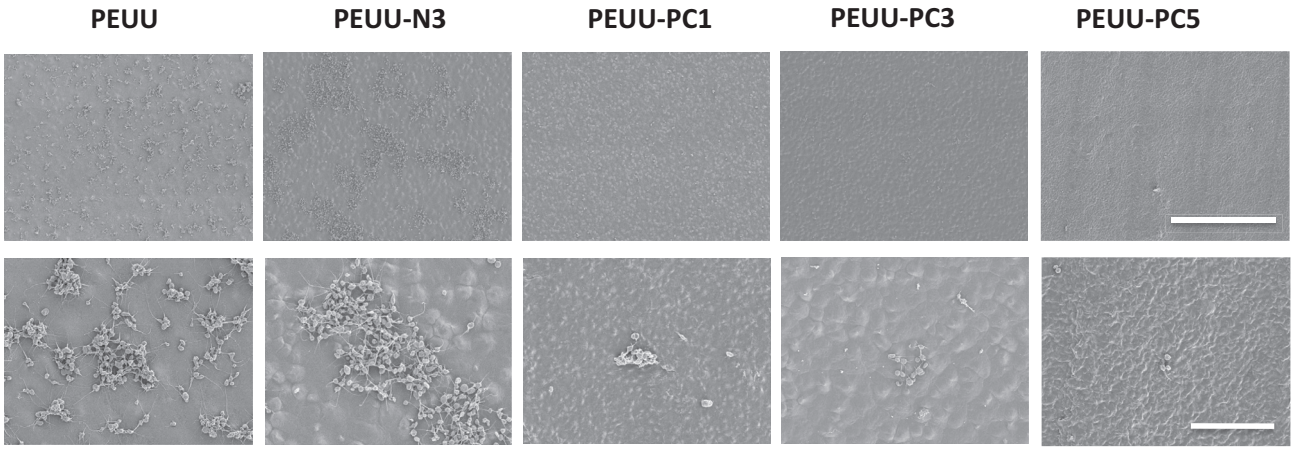

Fig. 7. Platelet adhesion (3 h contact with ovine blood) on cast films of PEUU, PEUU–N3, PEUU–PC1, PEUU–PC3, PEUU–PC5; scale bar = 50 μm top row, 10 μm bottom row.

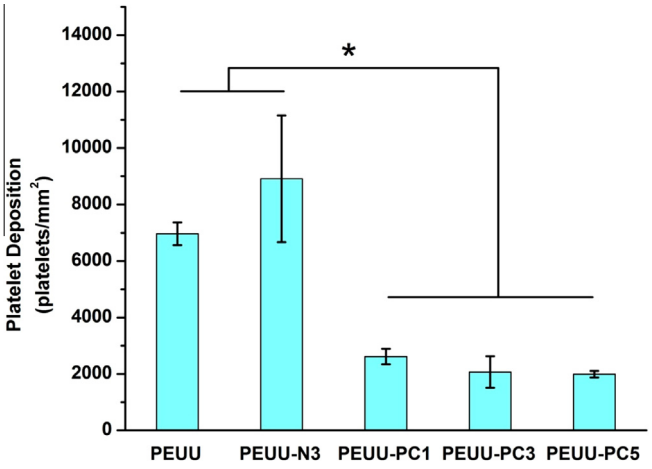

Fig. 8. Platelet deposition on cast films of PEUU, PEUU–N3, PEUU–PC1, PEUU–PC3, PEUU–PC5, quantified by LDH assay; $^{*}p < 0.05$.

activity. By day 4, all of the PEUU–PC surfaces had lower relative mitochondrial activity than the other surfaces and PEUU–PC3 and PEUU–PC5 were lower than PEUU–PC1.

4. Discussion

There have been other recent reports in the literature where the objective has been to design biodegradable polyurethanes incorporating functional groups, such as hydroxyl, alkyne and carboxyl, for subsequent modification. Yang et al. [27] have reported a biodegradable polyurethane containing free hydroxyl groups using benzyl pentaerythritol as a chain extender, followed by deprotection of the benzyl groups by CF_3COOH to generate the OH-containing polyurethanes. Song et al. [5] and Fournier and Du Prez [28] synthesized polyurethanes containing alkyne groups, which were then further modified by click chemistry. The current authors [29] have previously reported on the development of PEUU containing free carboxyl groups synthesized from dimethylolpropionic acid (DMPA), PCL diol, BDI and putrescine. This latter polymer has the

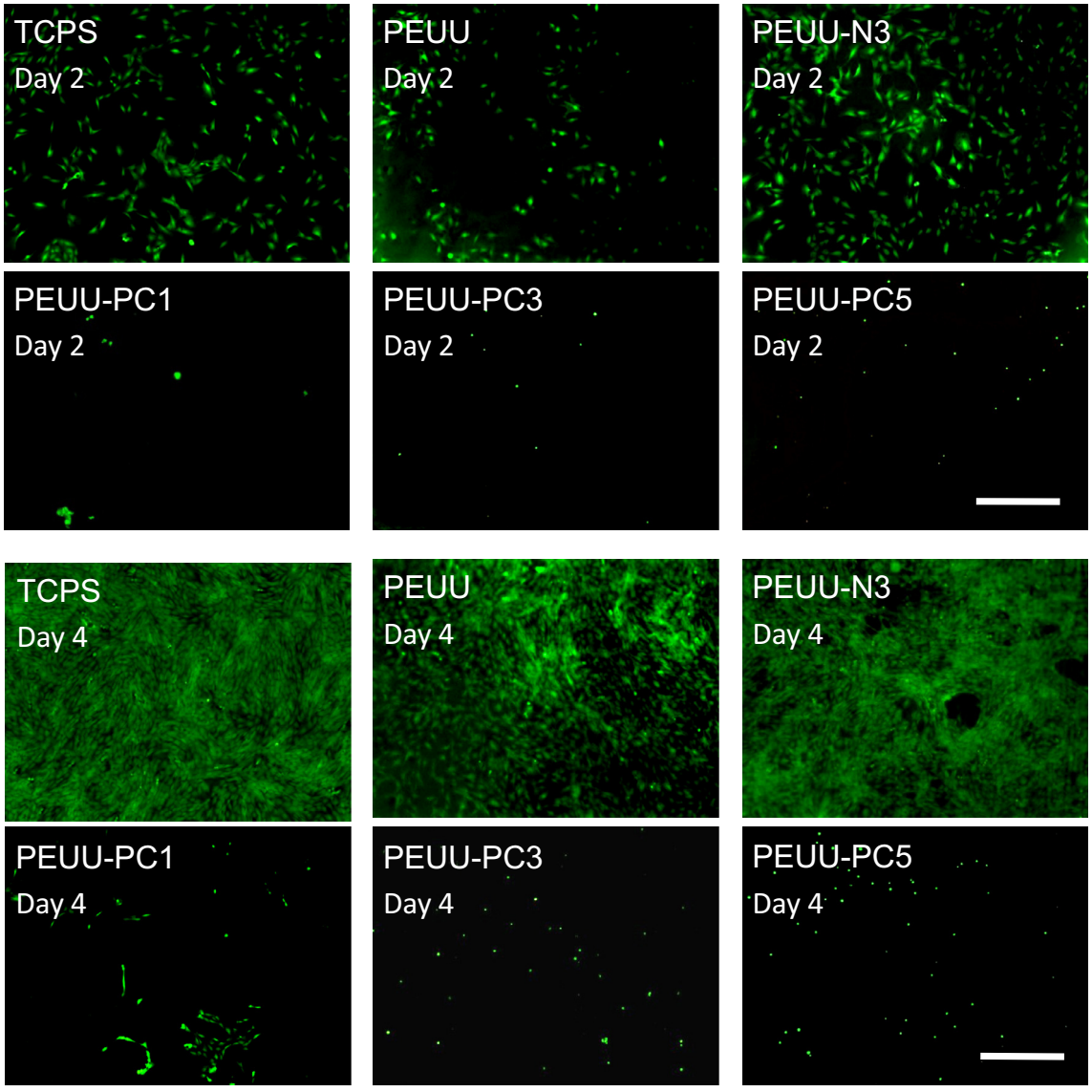

Fig. 9. Live/dead staining of rSMC on the polyurethane films at days 2 and 4. TCPS was utilized as a control; scale bar = 500 μm.

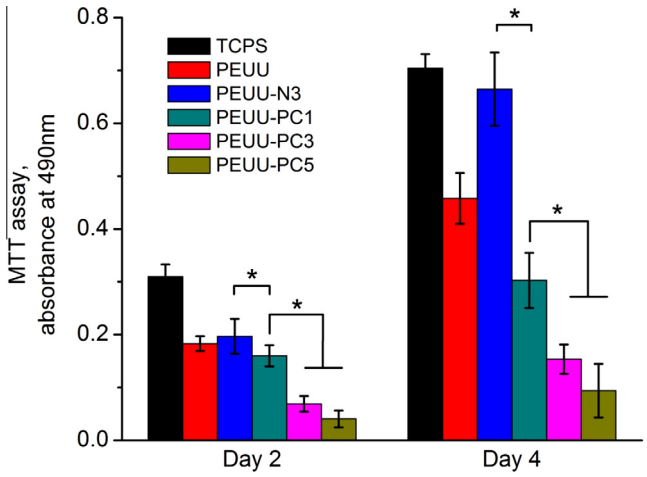

Fig. 10. MTT absorbance of rSMC on cast films of PEUU, PEUU–N3, PEUU–PC1, PEUU–PC3, PEUU–PC5 at days 2 and 4. TCPS was utilized as a control; $^{*}p < 0.05$.

disadvantage that the carboxyl group content is not protected during the initial synthesis and high carboxyl group content is not achievable.

In this study, a series of biodegradable PEUU elastomers containing variable amino group content were developed through a relatively easy and reproducible strategy using N-Boc-serinol together with PCL-diol in the first synthetic step. After deprotection of the Boc groups, and considering the serinol segments as part of the hard segments, the PEUU–NH_2 polymers would theoretically have hard segment contents in the range of 29–71 wt.%. For these polymers increasing hard segment content was associated with an increase in the initial modulus and decrease in the elongation at break (Table 2). Since bulk modification of a polymer can affect mechanical properties, the tensile behavior of the PEUU–NH_2 polymers with PC conjugation was examined. The results showed the same trend for PEUU–PC polymers. The strength at break was not affected by the percentage of hard segment content, although PEUU–PC polymers were 25–50% stronger than PEUU–NH_2. This latter phenomenon might be explained by ionic and hydrogen bonding interactions related to the PC side groups and also possibly greater chain entanglements [29]. Given the strengthening observed with the introduction of the PC groups, it does not appear that these groups acted to disrupt hard segment domain formation involving the chain extender, or at least were able to compensate for such disruptions. After water immersion, the mechanical properties of stress and strain at break and initial modulus were significantly decreased for all PC modified polyurethanes. This was likely due to water absorption weakening hydrogen bonding in the hard segment, an effect that became more pronounced with greater water absorption [30].

The mechanical properties of the PEUU–NH_2 polymers with relatively lower amino content (PEUU–N1, PEUU–N2, PEUU–N3) exhibited tensile properties similar to those of the previous reported PEUU (strain at break 660%, tensile strength 29 MPa) [25], which have shown promise after being processed into scaffolds for applications in abdominal wall repair [16], vascular tissue engineering [17] and right ventricular outflow tract replacement [19]. Although the wet mechanical properties of PEUU–PC polymers were weakened relative to the PEUU–NH_2 polymers, they still possessed greater breaking strength, elastic modulus and ultimate strain than those of native femoral arteries (tensile strength = 1–2 MPa, elastic modulus = 9–12 MPa, elongation at break = 63–76%) [31]. With suitable fabrication techniques [1,7,12] the PEUU–NH_2 and PEUU–PC polymers might thus warrant evaluation in subsequent studies as soft tissue engineering scaffolds.

The obtained T_g values for the soft segment in PEUU–NH_2 and PEUU–PC polymers were nearly constant at −60 °C. An earlier report with biodegradable polyurethanes utilizing polycarbonate soft segments instead of polyester has similarly noted that soft segment T_g values appeared to be independent of the hard segment content when this content was >30 wt.% [32]. Although the soft segments are different, both have a semi-crystalline character and the current data would be consistent with this earlier report in that for all of the PEUU–NH_2 polymers studied, the hard segment content was $\geqslant$29 wt.%. The endotherm due to the soft segment melting decreased as soft segment content decreased. This was likely due to the semi-crystalline character of the PCL soft segment being able to segregate to a greater extent and thus support microcrystalline domain formation with more soft segment content.

Water absorption of PEUU–NH_2 increased with increasing hard segment content, attributable to the increasing density of hydrophilic NH_2 groups. The water absorption for PEUU–NH_2 polymers increased after PC moiety grafting, due to the hydrophilicity of the PC moiety [33]. In relating the water absorption data to the degradation data, the results were generally as expected for incubation in buffered saline, with the most hydrophilic polymers showing significant mass loss at 16 weeks. The soft segment of poly(ether ester)urethane ureas has previously been manipulated to increase ether content, thus increasing hydrophilicity, and increase the degradation rate in aqueous buffer [7]. It was unexpected to find that the degradation in lipase solution, which might be expected to simply accelerate this degradation phenomenon, did not show faster degradation for PEUU–PC in lipase solution than in PBS, and that relative to the more hydrophobic PEUU–NH_2 polymers, those with the MPC modification degraded to a lesser extent. One interpretation of these data is that the expression of the PC moieties on the surface is markedly reducing protein adsorption, and thus the lipase enzyme is not able to adhere adequately with the polymer surfaces to act on the labile bonds in the exposed polymer segments.

It is also a limitation that the temporal changes in polymer molecular weight could not be measured due to the limited solubility of the polymers in common organic solvents used for gel permeation chromatography. It is possible that more substantial reductions in molecular weight preceding measurable mass loss would have been seen at earlier time points and with the PEUU–PC polymers.

Currently, the device-centered formation of occlusive thrombi and chronic development of neointimal hyperplasia remain leading causes for the failure of vascular stents [34] and small diameter synthetic vessels (<6 mm) [35]. Thromboresistance and the retardation of SMC proliferation are attractive design features for synthetic blood contacting materials. Myriad strategies have been developed to diminish platelet adhesion and SMC proliferation by the surface modification of polyurethanes, such as with PEG, heparin or albumin attachment, the seeding of endothelial cells or mesenchymal stem cells [36–38] and coating with zwitterionic groups including phosphorylcholine, sulfobetaine and carboxybetaine [22,24,39]. Smith et al. [39] developed a zwitterionic polymeric sulfobetaine surface modification for peripherally inserted polyurethane central catheters, showing effectiveness in reducing protein, mammalian cell and microbial attachment to putatively reduce thrombosis and infection in vivo. Gao et al. [40] grafted 2-methacryloyloxyethyl phosphorylcholine onto polycarbonate urethane surfaces by the Michael reaction to reduce platelet adhesion. In general, polymers presenting surface zwitterionic groups have been reported to exhibit reduced cellular affinity and this has been attributed to resistance to protein adsorption, limited plasma protein activation and the formation of a tightly bound hydration layer on the surface [41,42].

Although surface modification of polyurethanes for improved hemocompatibility is common in the literature, as noted above, fewer reports have sought to develop biodegradable polyurethanes with pendant reactive groups for subsequent bulk functionalization [27–29]. This latter approach is of particular relevance for degradable materials in that surface modifications would be expected to be shed in the early period of degradation, leaving unmodified surfaces at later time points which might support thrombosis and hyperplasia. In this study, we developed biodegradable polyurethanes with pendant amine groups for subsequent bulk functionalization. PC grafting markedly reduced platelet and smooth muscle cell adhesion with increased efficacy as PC density increased. The non-modified PEUU–N3 polymer experienced more platelet adhesion than PEUU, an effect that might be explained by the increased cationic nature of the amine containing polymer. This would be consistent with previous reports on amino-bearing surfaces being associated with increased protein adsorption and cell proliferation [43].

Several limitations of the current paper are worth noting. Most importantly, the synthesized materials have not been implanted into an animal model for an extended period of time. Contact with cells and blood only provide limited insight into how the materials might perform in a cardiovascular application. In particular, chronic thrombogenicity or resistance to hyperplasia could only be studied in vivo. Related to this limitation, the degradation properties in vivo are undefined. Whether the effect that was observed of reduced degradation in the presence of enzyme for the PEUU–PC polymers would be recapitulated in vivo is not known. The milieu of enzymes in vivo is extensive and the local presence of phagocytic, enzyme-releasing cells might lead to faster degradation profiles. Finally, it is worth mentioning the compromises in mechanical properties that come with the grafting of PC groups onto the PEUU–NH_2, particularly in a wet environment. While the grafted polymers remained elastic and would likely be mechanically compatible with many applications, the increased hydrophilicity increases swelling and reduces the tensile properties markedly.

5. Conclusions

Biodegradable PEUU elastomers with variable amino content were synthesized and characterized. The subsequent functionalization of these polymers with PC groups was achieved with increasing PC grafting at higher amino content, and platelet deposition and rSMC proliferation were significantly decreased with increased PC group conjugation. Looking forward, the synthesized PEUU–PC polymers may find utility as coatings in cardiovascular devices, such as stents, or as cardiovascular tissue engineering scaffold materials. The results also indicate the feasibility of functionalizing the PEUU–NH_2 with other specific bioactive molecules for a variety of biomedical applications.

Acknowledgements

This research was supported by the China Scholarship Council (201206630040), Fundamental Research Funds for the Central Universities (12D10631), National Nature Science Foundation of China (31271035, 31470941), Science and Technology Commission of Shanghai Municipality (11nm0506200) and The National Research Foundation for the Doctoral Program of Higher Education of China (20130075110005). This research was also supported by the NSF Engineering Research Center for Revolutionizing Metallic Biomaterials (ERC-RMB) (Award #0812348, National Science Foundation).We appreciate the XPS surface analysis provided by NESAC/BIO at the University of Washington (NIH grant EB 002027) and Prof. Kazuhiko Ishihara at the University of Tokyo for providing the MPC monomer. We would also like to thank the Center for Biological Imaging (CBI) at the University of Pittsburgh for their kind assistance with SEM imaging.

Appendix A. Figures with essential color discrimination

Certain figures in this article, particularly Figs. 1–6 and 8–10 are difficult to interpret in black and white. The full color images can be found in the on-line version, at http://dx.doi.org/10.1016/j.actbio.2014.08.008.

Appendix B. Supplementary data

Supplementary data associated with this article can be found, in the online version, at http://dx.doi.org/10.1016/j.actbio.2014.08.008.

References

[1] Chen Q, Liang S, Thouas GA. Elastomeric biomaterials for tissue engineering. Prog Polym Sci 2013;38:584.
[2] Guelcher SA. Biodegradable polyurethanes: synthesis and applications in regenerative medicine. Tissue Eng Part B Rev 2008;14:3.
[3] Cherng JY, Hou TY, Shih MF, Talsma H, Hennink WE. Polyurethane-based drug delivery systems. Int J Pharm 2013;450:145.
[4] Morral-Ruíz G, Melgar-Lesmes P, Solans C, García-Celma M. Multifunctional polyurethane–urea nanoparticles to target and arrest inflamed vascular environment: a potential tool for cancer therapy and diagnosis. J Control Release 2013;171:163.
[5] Song N, Ding M, Pan Z, Li J, Zhou L, Tan H, et al. Construction of targeting-clickable and tumor-cleavable polyurethane nanomicelles for multifunctional intracellular drug delivery. Biomacromolecules 2013;14:4407.
[6] Guan J, Sacks MS, Beckman EJ, Wagner WR. Biodegradable poly(ether ester urethane)urea elastomers based on poly(ether ester) triblock copolymers and putrescine: synthesis, characterization and cytocompatibility. Biomaterials 2004;25:85.
[7] Guan J, Fujimoto KL, Sacks MS, Wagner WR. Preparation and characterization of highly porous, biodegradable polyurethane scaffolds for soft tissue applications. Biomaterials 2005;26:3961.
[8] Santerre J, Woodhouse K, Laroche G, Labow R. Understanding the biodegradation of polyurethanes: from classical implants to tissue engineering materials. Biomaterials 2005;26:7457.
[9] Hong Y, Guan J, Fujimoto KL, Hashizume R, Pelinescu AL, Wagner WR. Tailoring the degradation kinetics of poly(ester carbonate urethane)urea thermoplastic elastomers for tissue engineering scaffolds. Biomaterials 2010;31:4249.
[10] Guan J, Wagner WR. Synthesis, characterization and cytocompatibility of polyurethaneurea elastomers with designed elastase sensitivity. Biomacromolecules 2005;6:2833.
[11] Skarja G, Woodhouse K. In vitro degradation and erosion of degradable, segmented polyurethanes containing an amino acid-based chain extender. J Biomater Sci Polym Ed 2001;12:851.
[12] Guan J, Stankus JJ, Wagner WR. Development of composite porous scaffolds based on collagen and biodegradable poly(ester urethane)urea. Cell Transplant 2006;15:S17.
[13] Hung KC, Tseng CS, Hsu Sh. Synthesis and 3D printing of biodegradable polyurethane elastomer by a water-based process for cartilage tissue engineering applications. Adv Healthc Mater 2014. http://dx.doi.org/10.1002/adhm.201400018.
[14] Niu Y, Chen KC, He T, Yu W, Huang S, Xu K. Scaffolds from block polyurethanes based on poly(ε-caprolactone) (PCL) and poly(ethylene glycol) (PEG) for peripheral nerve regeneration. Biomaterials 2014;35:4266.
[15] Gisselfält K, Edberg B, Flodin P. Synthesis and properties of degradable poly(urethane urea)s to be used for ligament reconstructions. Biomacromolecules 2002;3:951.
[16] Hong Y, Takanari K, Amoroso NJ, Hashizume R, Brennan-Pierce EP, Freund JM, et al. An elastomeric patch electrospun from a blended solution of dermal extracellular matrix and biodegradable polyurethane for rat abdominal wall repair. Tissue Eng Part C Methods 2011;18:122.
[17] Hong Y, Ye S-H, Nieponice A, Soletti L, Vorp DA, Wagner WR. A small diameter, fibrous vascular conduit generated from a poly(ester urethane)urea and phospholipid polymer blend. Biomaterials 2009;30:2457.
[18] Hashizume R, Hong Y, Takanari K, Fujimoto KL, Tobita K, Wagner WR. The effect of polymer degradation time on functional outcomes of temporary elastic patch support in ischemic cardiomyopathy. Biomaterials 2013;34:7353.
[19] Fujimoto KL, Guan J, Oshima H, Sakai T, Wagner WR. In vivo evaluation of a porous, elastic, biodegradable patch for reconstructive cardiac procedures. Ann Thorac Surg 2007;83:648.

[20] Jun H-W, Taite LJ, West JL. Nitric oxide-producing polyurethanes. Biomacromolecules 2005;6:838.
[21] Stachelek SJ, Finley MJ, Alferiev IS, Wang F, Tsai RK, Eckells EC, et al. The effect of CD47 modified polymer surfaces on inflammatory cell attachment and activation. Biomaterials 2011;32:4317.
[22] Baumgartner JN, Yang CZ, Cooper SL. Physical property analysis and bacterial adhesion on a series of phosphonated polyurethanes. Biomaterials 1997;18:831.
[23] Cao J, Yang M, Lu A, Zhai S, Chen Y, Luo X. Polyurethanes containing zwitterionic sulfobetaines and their molecular chain rearrangement in water. J Biomed Mater Res A 2013;101:909.
[24] Ma C, Zhou H, Wu B, Zhang G. Preparation of polyurethane with zwitterionic side chains and their protein resistance. ACS Appl Mater Interfaces 2011;3:455.
[25] Guan J, Sacks MS, Beckman EJ, Wagner WR. Synthesis, characterization, and cytocompatibility of elastomeric, biodegradable poly(ester-urethane)ureas based on poly(caprolactone) and putrescine. J Biomed Mater Res 2002;61:493.
[26] Tamada Y, Kulik EA, Ikada Y. Simple method for platelet counting. Biomaterials 1995;16:259.
[27] Yang L, Wei J, Yan L, Huang Y, Jing X. Synthesis of OH-group-containing, biodegradable polyurethane and protein fixation on its surface. Biomacromolecules 2011;12:2032.
[28] Fournier D, Du Prez F. "Click" chemistry as a promising tool for side-chain functionalization of polyurethanes. Macromolecules 2008;41:4622.
[29] Hong Y, Ye S-H, Pelinescu AL, Wagner WR. Synthesis, characterization, and paclitaxel release from a biodegradable, elastomeric, poly(ester urethane)urea bearing phosphorylcholine groups for reduced thrombogenicity. Biomacromolecules 2012;13:3686.
[30] Yang B, Huang W, Li C, Li L. Effects of moisture on the thermomechanical properties of a polyurethane shape memory polymer. Polymer 2006;47:1348.
[31] Hasan A, Memic A, Annabi N, Hossain M, Paul A, Dokmeci MR, et al. Electrospun scaffolds for tissue engineering of vascular grafts. Acta Biomater 2014;10:11.
[32] Eceiza A, Martin M, De La Caba K, Kortaberria G, Gabilondo N, Corcuera M, et al. Thermoplastic polyurethane elastomers based on polycarbonate diols with different soft segment molecular weight and chemical structure: mechanical and thermal properties. Polym Eng Sci 2008;48:297.
[33] Xu Y, Takai M, Ishihara K. Phospholipid polymer biointerfaces for lab-on-a-chip devices. Ann Biomed Eng 2010;38:1938.
[34] Zhang K, Liu T, Li JA, Chen JY, Wang J, Huang N. Surface modification of implanted cardiovascular metal stents: from antithrombosis and antirestenosis to endothelialization. J Biomed Mater Res A 2014;102:588.
[35] Seifu DG, Purnama A, Mequanint K, Mantovani D. Small-diameter vascular tissue engineering. Nat Rev Cardiol 2013;10:410.
[36] Amiji M, Park K. Surface modification of polymeric biomaterials with poly(ethylene oxide), albumin, and heparin for reduced thrombogenicity. J Biomater Sci Polym Ed 1993;4:217.
[37] Chuang T-W, Masters KS. Regulation of polyurethane hemocompatibility and endothelialization by tethered hyaluronic acid oligosaccharides. Biomaterials 2009;30:5341.
[38] Mirza A, Hyvelin J-M, Rochefort GY, Lermusiaux P, Antier D, Awede B, et al. Undifferentiated mesenchymal stem cells seeded on a vascular prosthesis contribute to the restoration of a physiologic vascular wall. J Vasc Surg 2008;47:1313.
[39] Smith RS, Zhang Z, Bouchard M, Li J, Lapp HS, Brotske GR, et al. Vascular catheters with a nonleaching poly-sulfobetaine surface modification reduce thrombus formation and microbial attachment. Sci Transl Med 2012;4:153.
[40] Gao B, Feng Y, Lu J, Zhang L, Zhao M, Shi C, et al. Grafting of phosphorylcholine functional groups on polycarbonate urethane surface for resisting platelet adhesion. Mater Sci Eng C 2013;33:2871.
[41] Chen S, Zheng J, Li L, Jiang S. Strong resistance of phosphorylcholine self-assembled monolayers to protein adsorption: insights into nonfouling properties of zwitterionic materials. J Am Chem Soc 2005;127:14473.
[42] He Y, Hower J, Chen S, Bernards MT, Chang Y, Jiang S. Molecular simulation studies of protein interactions with zwitterionic phosphorylcholine self-assembled monolayers in the presence of water. Langmuir 2008;24:10358.
[43] Chua K-N, Chai C, Lee P-C, Tang Y-N, Ramakrishna S, Leong KW, et al. Surface-aminated electrospun nanofibers enhance adhesion and expansion of human umbilical cord blood hematopoietic stem/progenitor cells. Biomaterials 2006;27:6043.